Zhang *et al. Carbon Research* (2025) 4:53
https://doi.org/10.1007/s44246-025-00219-3

Carbon Research

ORIGINAL ARTICLE

Open Access

Structure-performance relationship of biochar for direct degradation of organic pollutants

Fan Zhang[1], Yuan Gao[1*], Yajie Gao[1] and Rui Han[1]

Abstract

Recently, most of biochar materials are used as adsorbents to adsorb pollutants or as catalysts for oxidants (*e.g.* H_2O_2, persulfate, O_3) to degrade organic pollutants via free radical pathway and nonradical pathway. Actually, the property of electron transfer endows biochar with direct degradation capability, which is overlooked. However, the structure-performance relationship of biochar for direct degradation of organic pollutants still remains unclear. Besides, the distinction between adsorption, direct degradation, and indirect degradation is also very ambiguous. Therefore, this study employed quantification tests, electrochemical tests and correlation analysis to address this gap. The results show that both the direct and indirect degradation behavior occurred in the system of biochar with different types of organic pollutants. The direct degradation capacity of biochar was highly related to the electron-donating capacity. Additionally, the C–O groups, O–H groups, and graphitic structure promoted the electron transfer for the direct degradation of organic pollutants. Generally speaking, the direct degradation of biochar in our study reached up to 40% ± 10% in the whole degradation performance of both the direct and indirect degradation. Moreover, biochar maintained stable direct degradation performance even after five cycles (~ 100%). This study provides a new insight into the property of biochar in wastewater treatment, rather than adsorbent or catalyst.

Highlights

- Direct and indirect performance of biochar were distinguished and quantified.
- Direct degradation capacity is highly related to the electron-donating capacity.
- C–O groups, O–H groups, and graphitic structure promoted direct electron transfer.
- Oxygen competed with pollutant for electrons to hinder direct degradation.

Keywords Biochar properties, Direct degradation, Indirect degradation, Electron transfer

*Correspondence:
Yuan Gao
gaoyuan1988@dlut.edu.cn
[1]Key Laboratory of Industrial Ecology and Environmental Engineering (Ministry of Education), School of Environmental Science and Technology, Dalian University of Technology, Linggong Road 2, Dalian 116024, People's Republic of China

Graphical Abstract

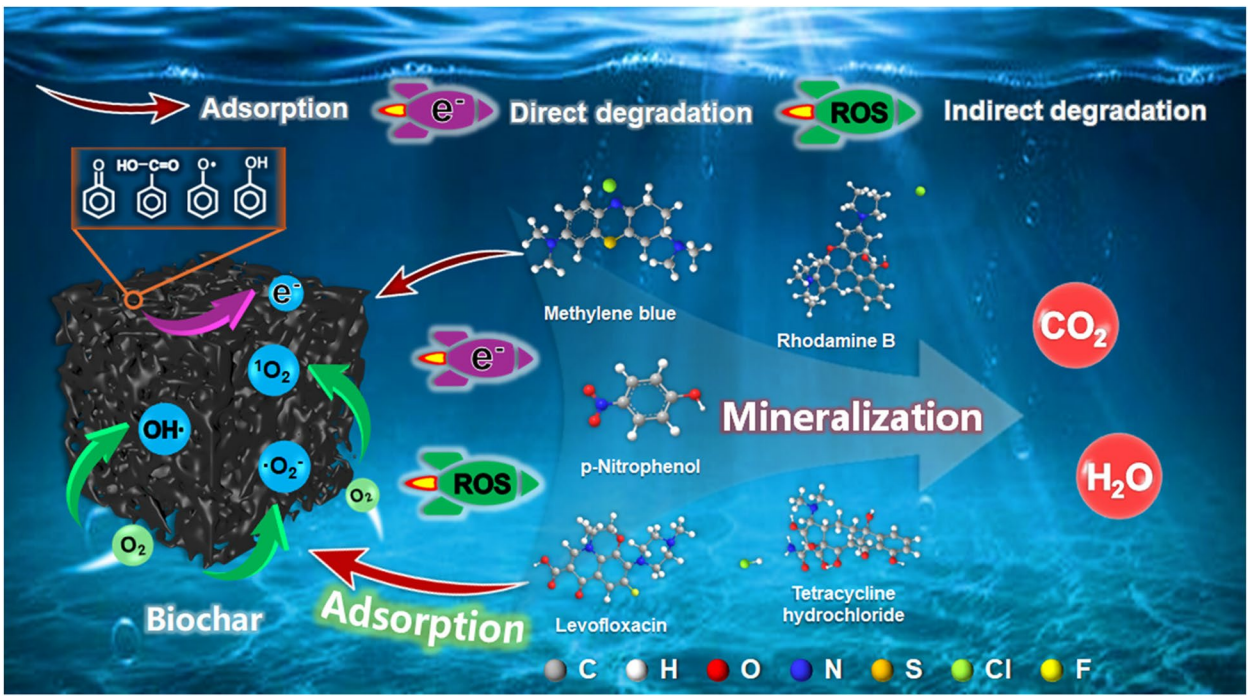

1 Introduction

Biochar is a low-cost and environmentally friendly material synthesized by the pyrolysis of biomass waste under low-oxygen conditions, which has gained attention in recent years. Until now, biochar materials are mainly used in two fields, namely adsorbent or catalysts (Beryani et al. 2025; Tian et al. 2025; Wang et al. 2025; Xiao et al. 2025; Zhang et al. 2023). On the one hand, biochar materials are usually applied as adsorbents to remove the pollutants from the wastewater. It is worth noting that regeneration or disposal of biochar is inevitable, when the biochar-based adsorbent reach saturation adsorption (Alsawy et al. 2022; Cui et al. 2022; Deng et al. 2023; Ouiriemmi et al. 2022; Wu et al. 2024). On the other hand, biochar materials are normally used as catalysts to active the oxidants to produce reactive oxygen species (ROS) (*e.g.* HO•, $SO_4^{\bullet-}$, $\cdot O_2^-$) for the degradation of organic pollutants in the traditional advanced oxidation processes (Feng et al. 2025; Kang et al. 2025; Liu et al. 2022; Yin et al. 2023). In most of the traditional advanced oxidation processes, the oxidants, such as H_2O_2, persulfate, O_3, are indispensable to degrade organic pollutants via a free radical pathway (Chen et al. 2024; Fang et al. 2017; Sun et al. 2023; Wu et al. 2023a, b; Zhang et al. 2021; Zhu et al. 2025a, b). Actually, biochar not only possesses the ability to adsorb or catalyze, but also has the potential to directly degrade the organic pollutants.

The direct degradation represents that the degradation of organic pollutants by biochar is owing to the direct electron transfer between biochar and organic pollutants without any oxidants for the production of free radicals. To date, the direct degradation of organic pollutants by biochar is a promising alternative method, which has been proved by several scholars (Feng et al. 2020; Yang et al. 2017; Zeng et al. 2021). For example, Bo Pan et al. found that *p*-nitrophenol pollutant could be directly degraded by biochar via electron donation (Chen et al. 2020; Wu et al. 2023a, b). They also found that the persistent free radicals in biochar played an important role in the degradation of organic pollutants (Yang et al. 2016). It can be assumed that the oxidants could be saved if the direct degradation capacity of biochar can be controlled reasonably. According to the previous studies, it can be concluded that the performance of biochar in adsorption or catalysis relies on its physicochemical properties, such as porous structure, specific surface area, graphitization degree, surface functional groups. What's more, the vast majority of researches concluded that the high removal capacity of biochar-based materials towards organic pollutants was derived from the adsorption, which seems

to have overlooked the roles of direct degradation (Guo et al. 2023; Mon et al. 2023; Shao et al. 2023; Yang et al. 2025a, b; Zhang et al. 2024a, b). Therefore, it is interesting and necessary to figure out the structure-performance relationship of biochar for direct degradation of organic pollutants.

In conclusion, the main objective of this study was to elucidate the deep relationship between the biochar characteristics and the direct degradation performance of biochar without any oxidants, even including dissolved oxygen in natural aquatic system. Firstly, the contributions of pure adsorption, direct degradation, and indirect degradation were distinguished in the traditionally so-called "adsorption process". In this work, the pure adsorption means the removal of organic pollutant via adsorption without any transformation. The indirect degradation was due to the removal of organic pollutant by free radicals, which was derived from the activation of dissolved oxygen in wastewater by biochar. Secondly, the structure-performance relationship of biochar for direct degradation was revealed by characteristic analysis, electrochemical tests and correlation analysis. Finally, the direct degradation mechanism and cycling stability were concluded. This study will provide a new understanding about the role of biochar for the removal of organic pollutants.

2 Materials and methods

2.1 Materials and chemicals

P-nitrophenol (PNP), levofloxacin (LEV), tetracycline hydrochloride (TC), methylene blue (MB), and rhodamine b (RhB) were purchased from Aladdin Biochemical Technology Co., Ltd. Ammonium polyphosphate (APP) was purchased from Da Mao Chemical Co., Ltd. Acetonitrile (ACN), furfural (EtOH), tert-butanol (TBA), isopropanol (IPA), and furfuryl alcohol (FFA) were purchased from China National Pharmaceutical Group Chemical Reagent Co., Ltd.

2.2 Preparation of biochar

In order to produce biochar with tailored physicochemical characteristics, ammonium polyphosphate (APP) was used as a modified agent in this study. The reasons why APP was selected was owing to their advantages compared to the traditional modified agents, including low pyrolysis temperature, needless of inert gases protection, and low corrosivity. For example, the application of potassium hydroxide normally requires the protection of inert gases and heavy corrosion to the pyrolysis equipment. APP solution with a mass fraction of 25% was prepared by using APP at a polymerization degree of 50. Subsequently, 10 g of coconut shell samples were mixed with APP at varying ratios of 1:0, 1:0.25, 1:0.5, 1:0.75, 1:1, and 1:1.25. The mixtures were magnetically stirred for 24 h to ensure uniform loading of APP on biochar precursor. After impregnation, the samples were transferred to a muffle furnace. The pyrolysis was performed under 500 °C with a heating rate of 10 °C/min and held for 1 h. The resulting products were washed with deionized water until the pH of leachate reaching ~7, and dried at 60 °C with a vacuum oven. Finally, the biochar samples were obtained by sieving through a 100-μm mesh and labeled as APP-1 to APP-6.

2.3 Characterizations of biochar

The surface element compositions and functional groups of biochar were detected by X-ray photoelectron spectroscopy (XPS) (K-Alpha +, USA) under ultrahigh vacuum, scanning the binding energy range of 0–1200 eV (0.1 eV step size). Fourier-transform infrared spectroscopy (FTIR, Thermo Scientific Nicolet 6700, USA) was used to detect the changes in functional groups of biochars before and after the reaction. FTIR was conducted at a resolution of 4 cm^{-1} over a scanning range of 4000–400 cm^{-1} using a KBr beam splitter with 32 accumulated scans. The graphitization degree of biochars was measured by Raman spectroscopy (inVia Qontor, England) at an excitation laser wavelength of 532 nm with a spectral resolution of 1 cm^{-1}. N_2 adsorption–desorption measurements were performed at 77 K using a Quantachrome AS-1-MP-11 analyzer. Samples were degassed at 200 °C for 5 h before analysis. The BET method (P/P_0 = 0.05–0.30) was used for surface area calculation.

2.4 Degradation performance identification

To investigate the degradation performance of biochar on organic pollutant, the experiment was divided into two groups. One group introduced N_2 into the solution to create an anaerobic environment, while the other group maintained an aerobic environment without introducing N_2. Additionally, the quenching experiments were carried out to distinguish the roles of direct degradation and indirect degradation. In this study, the radical trapping agents included tert-butanol (TBA, 10 mM) for hydroxyl radicals (·OH), isopropanol (IPA, 10 mM) for singlet oxygen ($^1O_2$), and furfuryl alcohol (FFA, 1 mM) for superoxide radicals ($\cdot O_2^-$). To ensure the reliability and applicability of the results, three representative categories of organic pollutants were selected based on their structural diversity and environmental persistence: phenolic compounds p-nitrophenol (PNP), antibiotics levofloxacin (LEV) and tetracycline hydrochloride (TC), and dyes methylene blue (MB) and rhodamine B (RhB). For each reaction, 0.1 g of biochar was mixed with 100 mL of organic pollutant solution (200 ppm) in sealed containers. After sealing, the containers were transferred to a

shaker (25 ℃, 220 rpm) and agitated for 24 h in the dark. All solutions were freshly prepared to eliminate potential interference from microorganisms and other substances that could affect experimental results. Afterwards, the mixture was vacuum-filtered through a 0.22-μm nylon membrane. The filtrate was collected for quantification analysis via high-performance liquid chromatography (HPLC; Agilent 1260) using a C18 column (5-μm, 4.6 mm × 250 mm). And the biochar was recovered from the filter membrane, rinsed with deionized water (3 × 50 mL), and vacuum-dried at 60 °C for 12 h. External calibration curves (0.1–100 mg/L, $R^2 > 0.995$) ensured accuracy. Detailed methods are provided in Supplementary Text S2. Liquid chromatography-mass spectrometry (LC-MS; m/z 50–1000, positive ion mode) identified degradation intermediates. The degradation experiment was repeated five times. The details of electrochemical tests for electron transfer can be found in Text S3. All experiments were conducted in triplicate. Error bars indicate standard deviation ($n = 3$), with relative standard deviations < 5%. Statistical significance ($p < 0.05$) was confirmed by one-way ANOVA, ensuring robust conclusions.

3 Results and discussion

3.1 Overall removal performance of organic pollutants by biochar

Through the regulation of APP loading ratio, biochars with tailored physicochemical characteristics were produced, such as the total specific surface area (Table 1). Notably, the specific surface area of samples increased with the increasing APP loading ratio. Among them, APP-6 reached 134.8 m^2/g, representing an 8.2-fold increase compared to the unmodified biochar. Figure S1 shows the overall removal performances of the five organic pollutants by biochars, including pure adsorption, direct degradation, and indirect degradation. As shown in Fig. S2, there was a positive linear correlation between the change of BET surface area and total removal capacity ($R^2 = 0.89$). By comparing the porous structures of biochar before and after reaction, it can be concluded that the pore filling played an important role for the removal of organic pollutants. After five cycles, the overall removal performances of biochar decreased owing to the lack of reaction active sites.

Table 1 Total specific surface area of biochars APP-1 ~ APP-6 before and after reaction

Sample	Before reaction S_{BET} (m^2/g)	After reaction S_{BET} (m^2/g)
APP-1	16.43	0.13
APP-2	25.35	0.26
APP-3	37.28	0.53
APP-4	67.92	2.21
APP-5	117.88	7.08
APP-6	134.8	11.16

S_{BET} is total specific surface area

To demonstrate the presence of degradation behavior, LC-MS analysis was performed to check the pollutant species after reaction. It can be found from Fig. 1 that the generation of intermediates occurred for all five organic pollutants, including p-nitrophenol, levofloxacin, tetracycline hydrochloride, methylene blue, and rhodamine B. For instance, PNP was transformed into p-aminophenol (C_6H_7NO, m/z = 109.023) and phenol (C_6H_6O, m/z = 95.050). No intermediates were detected in blank controls, confirming that the degradation activity was derived from biochar. Notably, the degradation products were still observed even under strict anaerobic conditions, demonstrating the existence of direct degradation by biochar. The degradation efficiency was calculated by subtracting the adsorbed pollutant amount from the total removal (Fig. 2). To quantify the adsorption capacity, biochar was subjected to acetonitrile extraction (5 × 2 h extraction, 97% extraction efficiency), followed by HPLC analysis of the eluate. This method enabled differentiation between adsorption-driven removal and catalytic degradation-driven removal (Chen et al. 2020; Wu et al. 2022). According to the calculation, the pure adsorption contributed to about 70% ± 10% for overall removal performance, and the degradation contributed to approximately 30% ± 10% for overall removal performance. As above-mentioned, the degradation included both the direct and indirect degradation. Therefore, the contributions of these dual pathways were quantitatively elucidated by ROS quenching experiments and correlation analyses.

3.2 Indirect degradation of organic pollutants by biochar

Quenching experiments revealed the contribution of ROS to the degradation of organic pollutant by biochars (Fig. 3). The results demonstrated that ·OH and $^1O_2$ were the primary contributors to the indirect degradation, accounting for the maximum degradation capacities of 8.3 mg/g (28.5%) and 7.7 mg/g (24.9%), respectively. In other words, biochar could catalyze dissolved oxygen in natural water to produce ROS for the degradation of organic pollutants. Additionally, it can be observed that there was still degradation behavior after the quench of all ROS in the system, suggesting the presence of other degradation mechanism, rather than only the roles of ROS. After the five-cycle reaction, the degradation of ROS gradually decreased. In each cycle, the ratio of ROS degradation to the total degradation of organic pollutants reduced (Table 2), indicating that the ability of biochar

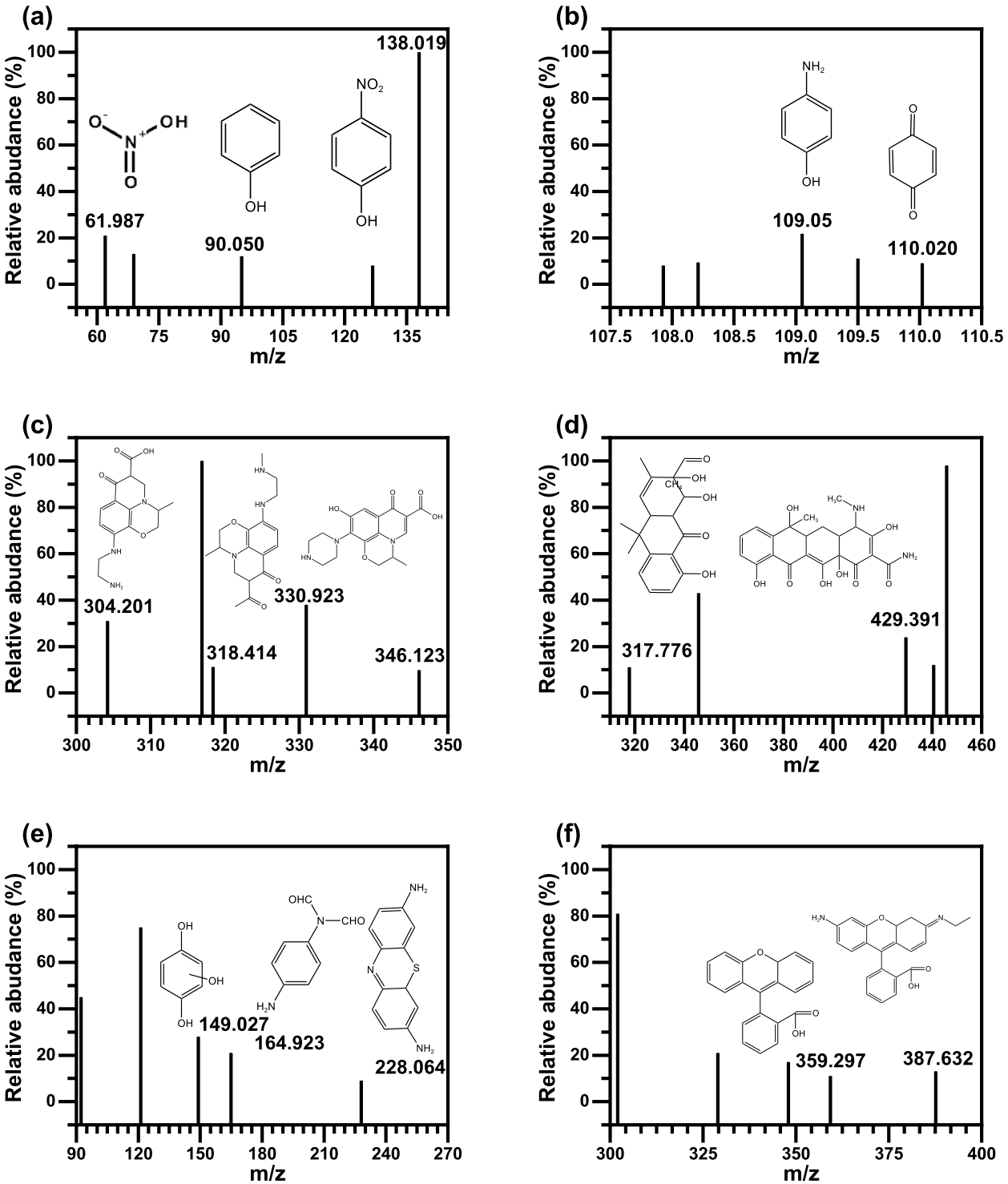

Fig. 1 LC–MS analysis of the solution after reaction and its corresponding degradation process of (**a**-**b**) PNP, (**c**) LEV, (**d**)TC, (**e**) MB, (**f**) RhB

to catalyze the generation of ROS gradually weakened. This phenomenon can be attributed to the consumption of biochar during the reaction process. According to the literatures (Dong et al. 2024; Li et al. 2022a, b, 2023a; Yang et al. 2025a, b; Zhang et al. 2024a, b), the surface oxygen-containing functional groups (O–H and C–O groups) in biochar could activate the dissolved oxygen to generate $^1O_2$ even under light-independent conditions.

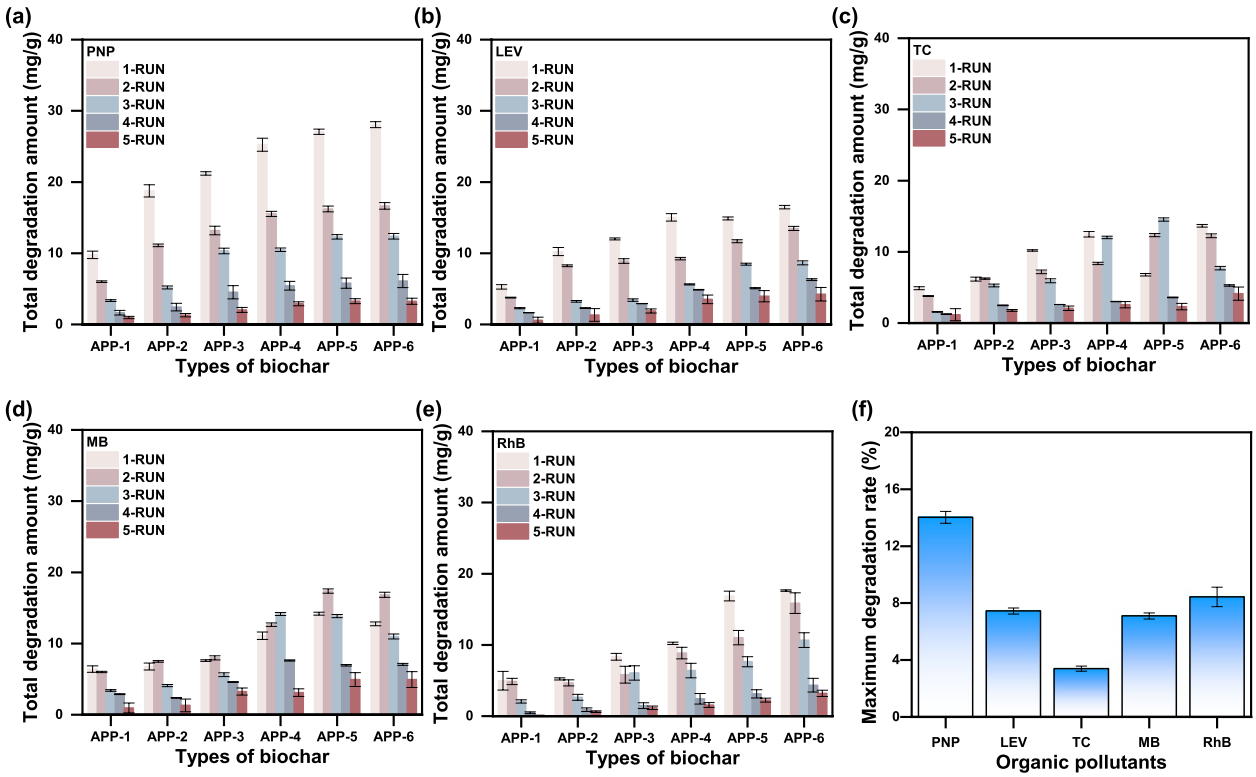

Fig. 2 The degradation effect of biochars on 200 ppm of (**a**) PNP, (**b**) LEV, (**c**) TC, (**d**) MB, and (**e**) RhB; (**f**) the maximum degradation rate of organic pollutants

Specifically, these surface functional groups acted as redox-active sites to capture the electrons and transfer them to O_2 to form $\cdot O_2^-$ (Zhu et al. 2025). Subsequently, $^1O_2$ could be produced via dismutation reaction in the presence of protons, and the protons were provided by O–H groups via hydrogen bonding. Besides, some researchers found that the persistent free radicals in biochar could activate and motivate the direct excitation of ground-state oxygen to highly reactive $^1O_2$ through energy transfer mechanisms (Fu et al. 2024; Li et al. 2022a, b).

3.3 Direct degradation of organic pollutants by biochar

In order to investigate the direct degradation performance of biochar, the removal experiments in either anaerobic (N_2) and natural condition (original dissolved oxygen) were performed. The direct degradation behaviors of PNP by biochars under two different conditions are compared in Fig. 4, and the degradation results of the other four organic pollutants are provided in Fig. S3. The results demonstrated the presence of degradation of organic pollutants, even under the anaerobic condition, during which the ROS could not be produced. Namely, the direct degradation of organic pollutants by biochar really existed. Furthermore, the direct degradation efficiency under anaerobic condition was lower than in the natural condition, indicating that both the direct and indirect degradation contributed to the removal of organic pollutants. The poor performance of direct degradation under aerobic conditions compared to anaerobic conditions also indicated that the presence of dissolved oxygen may compete with the organic pollutants for electrons from biochar. The ability of direct degradation of PNP by biochar gradually weakened with the increasing cycle numbers, which may be due to the gradual consumption of redox sites in biochar.

To further prove the direct degradation, the electrochemical tests were performed to investigate the electron transfer properties of biochar samples using a three-electrode system. As shown in Fig. 5, the linear sweep voltammetry curves (LSV) of all six biochar samples changed, accompanied by an increase in current intensity after the introduction of organic pollutants (Chu et al. 2022; Huang et al. 2023, 2025). This result indicated that biochar directly mediated the electron transfer at the pollutant interface, thereby achieving direct degradation of organic pollutants. What's more, the capacity of electron transfer enhanced from APP-1 to APP-6. The presence of electron transfer processes in the biochar-organic pollutant system revealed a possible relationship

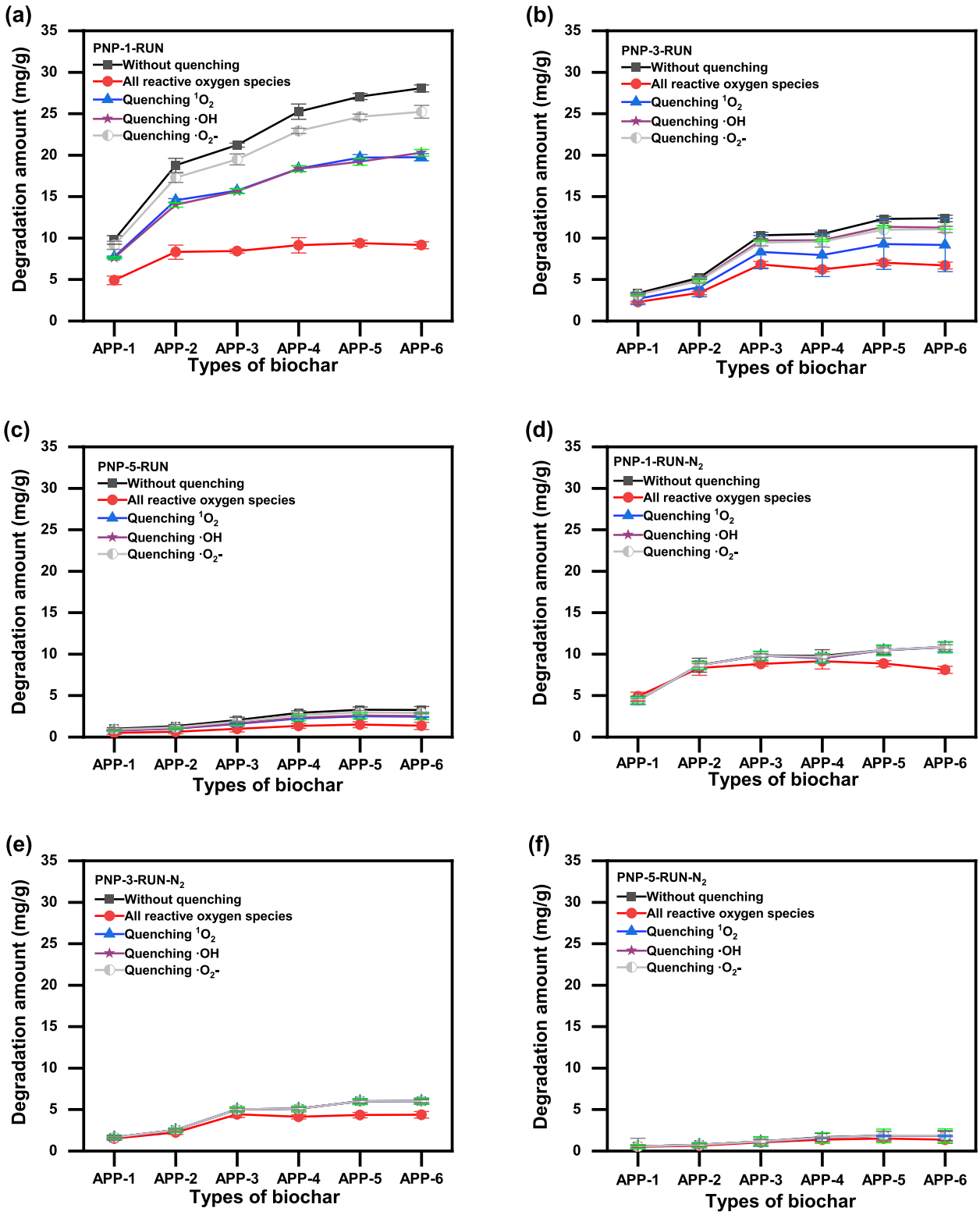

Fig. 3 Degradation of PNP by biochars under quenching conditions in (**a**), (**d**) 1-Run, (**b**), (**e**) 2-Run, and (**c**), (**f**) 3-Run

Table 2 The proportion of reactive oxygen species degradation in the total degradation amount (%)

Sample	The proportion of reactive oxygen species degradation in the total degradation amount (%)				
	1-Run	2-Run	3-Run	4-Run	5-Run
APP-1	63.70	60.70	55.20	52.60	50.50
APP-2	63.57	59.47	57.20	56.60	51.05
APP-3	64.96	61.02	58.72	55.47	51.95
APP-4	67.70	62.67	60.72	57.67	54.05
APP-5	66.00	61.68	59.72	59.66	54.40
APP-6	68.20	67.65	59.95	61.66	58.50

between the direct degradation capability of biochar and its electron transfer capacity. To quantitatively evaluate the kinetics of direct electron transfer during the redox reactions, this study employed a three-electrode system based on mediated electrochemical redox method. The experimental data in Table 3 reveal that electron-donating capacity (EDC) of biochars was significantly higher than their electron accepting-capacity (EAC) (Chen et al. 2022; Gorski et al. 2012; Govindan et al. 2020; Hoving et al. 2017). EDC was the main factor driving biochar's electron transfer capability, indicating that the direct degradation by biochar was predominantly governed by reductive processes. Notably, both the EDC and EAC of biochar samples gradually increased from APP-1 to APP-6, implying the possible improved electron transfer capacity for the degradation of organic pollutants.

3.4 Direct degradation mechanism of biochar

To elucidate the electron transfer mechanism, the characteristics of biochars before and after the reaction are

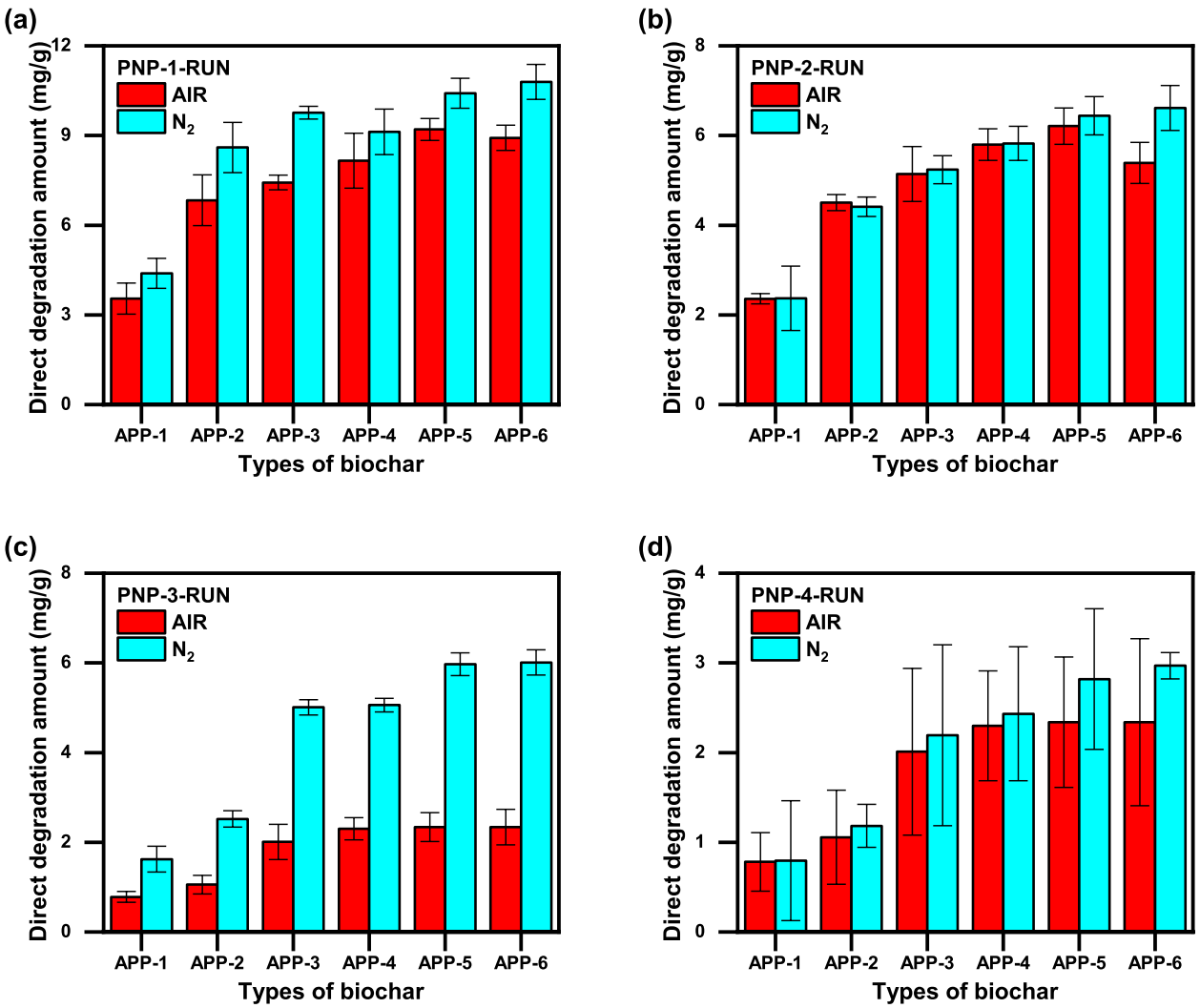

Fig. 4 Direct degradation of PNP by biochars in reactions of (**a**) 1-Run, (**b**) 2-Run, (**c**) 3-Run, and (**d**) 4-Run

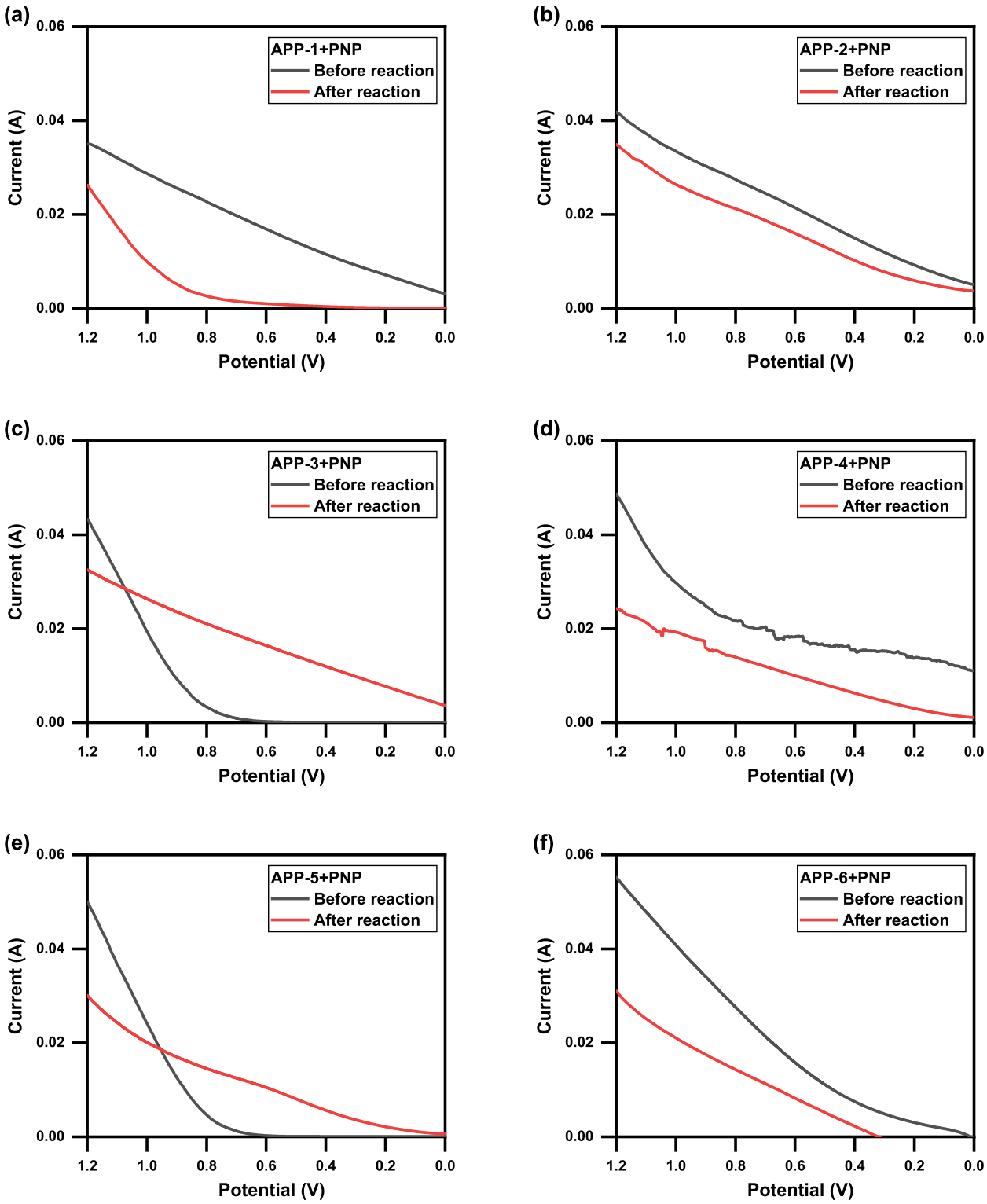

Fig. 5 Linear sweep voltammetry results of biochars (**a**-**f**) APP-1 ~ APP-6

Table 3 EDC, EAC and EEC of biochars APP-1 ~ APP-6

Sample	EDC (mmol e^-/g)	EAC (mmol e^-/g)	EEC (mmol e^-/g)
APP-1	0.006783	0.001802	0.008585
APP-2	0.016173	0.002452	0.018625
APP-3	0.024735	0.003001	0.027736
APP-4	0.029533	0.003284	0.032817
APP-5	0.034129	0.004601	0.038730
APP-6	0.041565	0.004984	0.046549

necessary. FTIR results confirmed the presence of O–H and C–O bonds in biochar, with stretching vibrations observed at 3430 cm^{-1} and 1000–1300 cm^{-1}, respectively (Fig. 6). Notably, the abundance of C–O and O–H bonds gradually increased from biochar APP-1 to APP-6 according to FTIR peaks and XPS (Table 4) (Egyir et al. 2022; Li et al. 2024; Zhu et al. 2025a, b). After the reaction, the intensity of surface functional groups in biochar decreased, indicating their participation in the removal reaction of organic pollutants. Therefore, it could be demonstrated that the surface functional groups my involve in the direct degradation of organic pollutants. The XPS data revealed the significant changes in the composition of biochars before and after the reaction, highlighting their roles in the removal process of pollutants (Figs. 7 and S4). Before the reaction, the content of C–C/C–H bonds progressively decreased from APP-1 (72.07%) to APP-6 (43.26%), while the oxygen-containing functional groups (C–O and O–H) showed a significant increase, with C–O rising from 6.22% to 66.59% and O–H from 6.89% to 48.28%. After the reaction, the C–C/C–H content increased across all samples, while the C–O and O–H content decreased substantially, with C–O dropping to 3.92%–31.92% and O–H to 4.21%–32.15%. Notably, the emergence of a new C=O stretching vibration peak was observed after the reaction, indicating the formation of carbonyl groups during the degradation process. Among the six biochar samples, APP-6 exhibited the most significant changes with the highest initial C–O (66.59%), O–H (48.28%) content and the largest post-reaction C=O formation (13.4%), reflecting their donation in electrons. This result was consistent with its highest direct degradation efficiency. The C–O and O–H groups acted as electron donors, driving the degradation of organic pollutants through direct electron transfer mechanisms. This process involved the transfer of electrons from the oxygen-containing functional groups on biochar to pollutants, facilitating the reductive transformations of the organic pollutants. These findings underscored the critical role of oxygen functional groups in biochar's redox activity, while also illustrated the structural differences among the six biochar samples and their varying contributions to the degradation process.

Raman spectroscopy was used to analyze the graphitization degree of biochar. Two characteristic peaks were observed at approximately 1350 cm^{-1} and 1580 cm^{-1}, corresponding to the D band (disordered sp^3-bonded carbon) and the G band (ordered sp^2-bonded carbon), respectively. The I_D/I_G ratios for APP-1 to APP-6 were 0.832, 0.836, 0.774, 0.868, 0.861, and 0.882. After the reaction, all six biochar exhibited the change of structural defects, which may serve as redox-active sites for both the adsorption and degradation of organic pollutants (Hou et al. 2022; Liang et al. 2021; Miao et al. 2022; Wang et al. 2019). These defect-driven interfaces facilitated the electron transfer between the biochar and pollutant molecules, thereby promoting the direct degradation capability of biochar.

3.5 Structure-performance relationship analysis

To further elucidate the relationship between biochar's structural properties and the degradation performance, a comprehensive correlation analysis was conducted in this study (Fig. 8). The results in Fig. S5 revealed that the BET surface area exhibited a relatively low correlation with direct degradation (R^2 = 0.624), indicating that physical adsorption played an indirect role in direct degradation of biochars. Instead, the degradation of organic pollutants relied on chemical reactivity of biochar, particularly the electron transfer capacity. Specifically, the direct degradation capability of biochar showed a positive correlation with EDC (R^2 = 0.867). The electron-exchanging capacity (EEC) is the sum of EAC and EDC, which also had a strong correlation with direct degradation (R^2 = 0.875). These findings suggested that biochar predominantly served as an electron donor, directly reducing pollutants through electron transfer. The changes in surface functional groups of biochar before and after reaction showed a significant correlation with its EDC. This also revealed the transformation relationship between C–C and C=O, as well as the connection between C=O and EDC. The correlation between O–H and EDC was 0.903, while the correlation between C–O and EDC was 0.947, indicating that the electron-donating capacity of biochar primarily derived from the groups O–H and C–O. The correlation between the changes in C–C and C=O groups was 0.754, indicating that the newly formed C=O may originate from the oxidative cleavage of C–C. During the removal process, the organic pollutants may oxidize the C–C bond, resulting in the formation of C=O functional groups. The correlation between C=O and EDC was 0.788, indicating that the formation of C=O was closely related to the electron-donating capacity of biochar. The generation of C=O may result from oxidation reactions

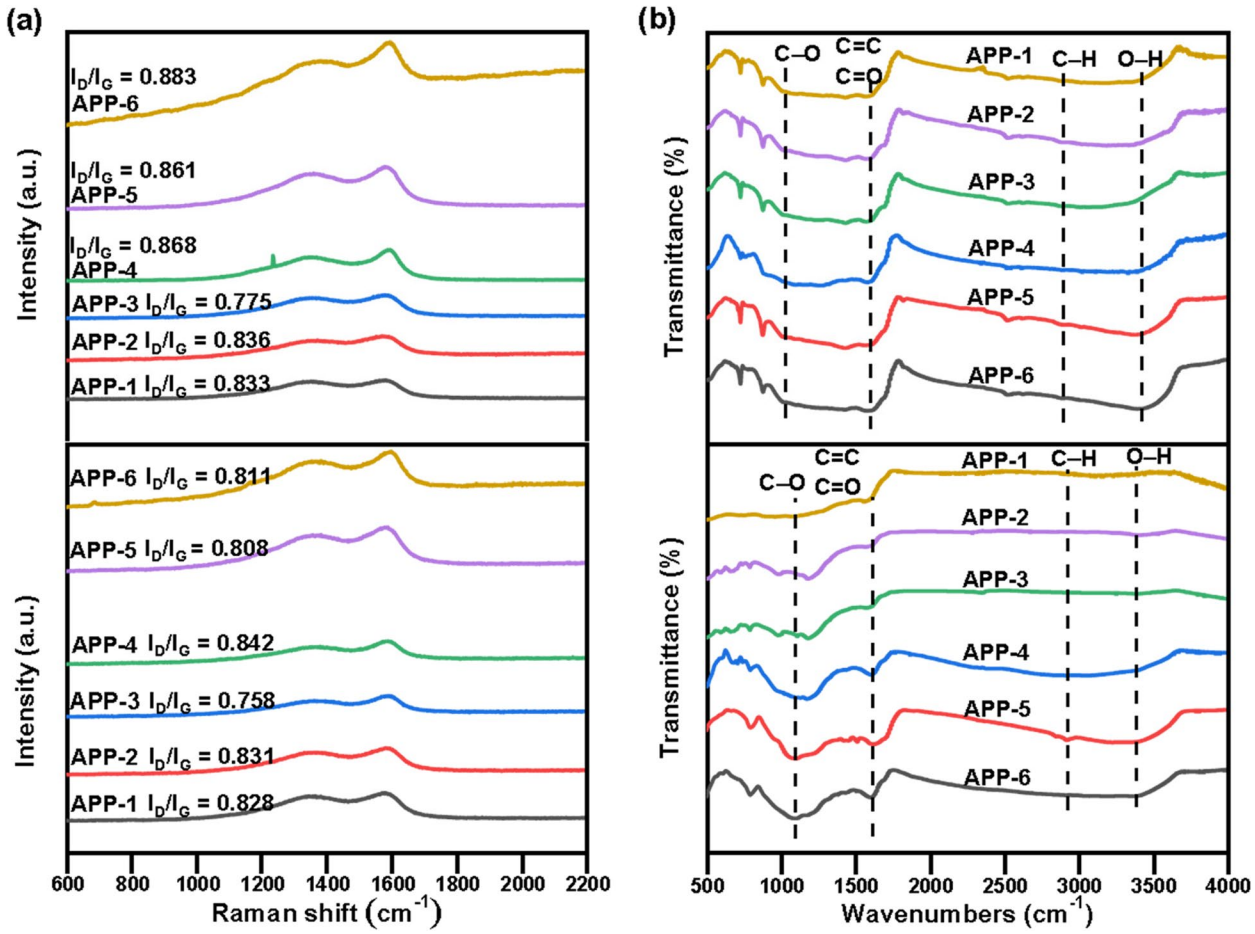

Fig. 6 Raman spectra of biochars APP-1 to APP-6 (**a**) before reaction, (**b**) after reaction; FTIR spectra of biochars APP-1 to APP-6 (**c**) before reaction, (**d**) after reaction

during the electron donation process, further supporting the electron donor characteristics of biochar. The changes in surface functional groups of biochar before and after reactions were significantly correlated with the direct degradation of organic pollutants. This indicated that the degradation mechanism of biochar relied on its electron donor characteristics, rather than only physical adsorption. The electron donor properties of surface functional groups (O–H, C–O) were important for the degradation of organic pollutants. The correlations of the changes in Raman spectra before and after the reaction with the direct degradation and EDC were 0.710 and 0.871, respectively, further highlighting the important influence of graphitic structure of biochar on its electron-donating capacity.

Based on all above-mentioned results, the degradation mechanism of organic pollutants by biochar was summarized and illustrated in Fig. 9, including both direct

Table 4 XPS C1 s and O1 s dates of biochars APP-1 ~ APP-6

Sample	Before reaction			After reaction			
	C–C/C–H (%)	C–O (%)	O–H (%)	C–C/C–H (%)	C–O (%)	O–H (%)	C=O (%)
APP-1	72.07	6.22	6.89	74.41	3.92	4.21	3.67
APP-2	68.04	27.09	16.58	78.11	13.2	8.51	7.36
APP-3	65.64	49.36	24.36	79.46	31.92	13.2	11.61
APP-4	61.02	58.36	29.35	75.51	27.86	15.62	10.63
APP-5	52.93	61.63	32.37	78.37	24.57	16.84	11.06
APP-6	43.26	66.59	48.28	74.34	21.26	32.15	13.4

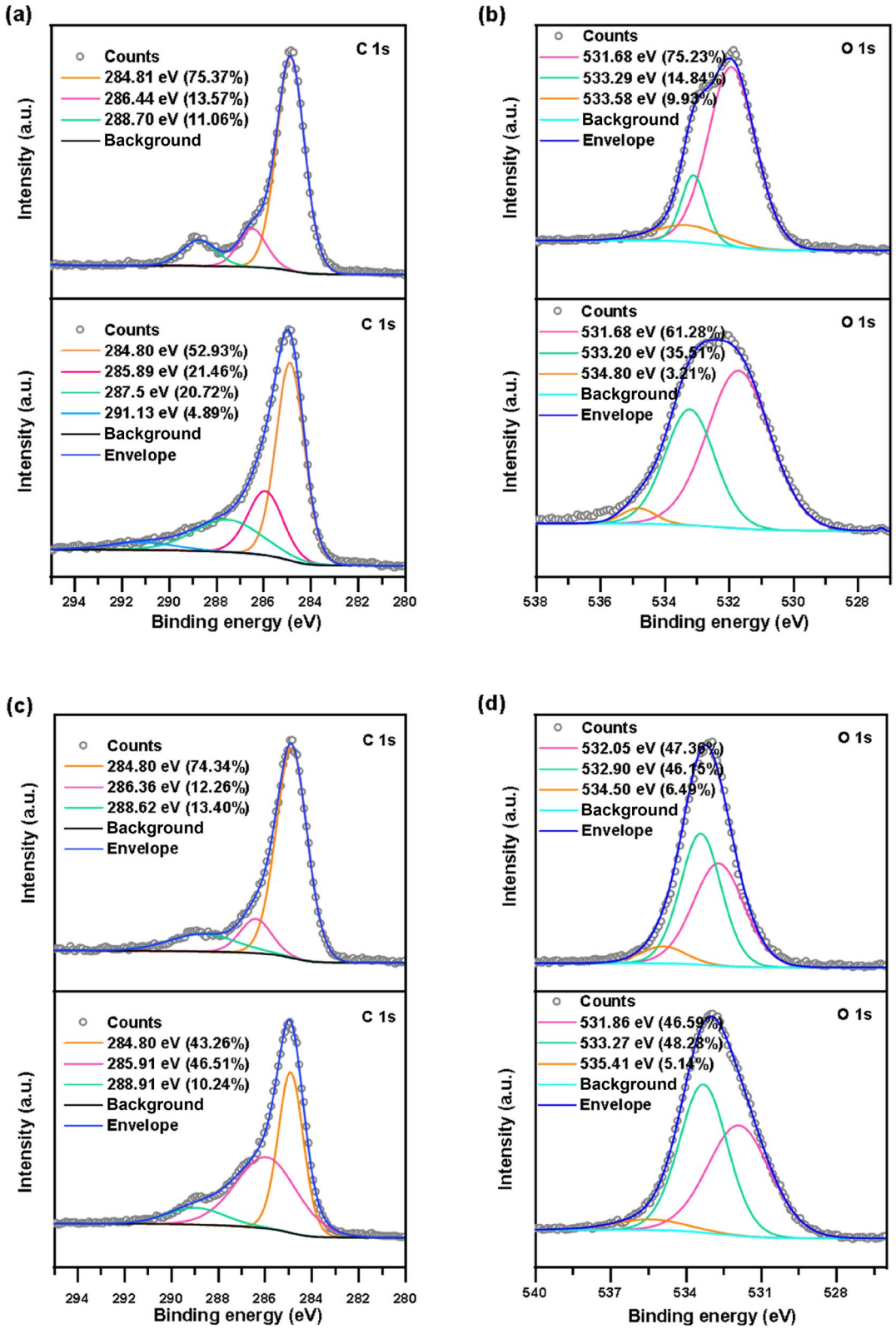

Fig. 7 (**a**), (**b**) C 1 s and (**c**), (**d**) O 1 s spectra of biochars APP-5, APP-6 before and after reaction

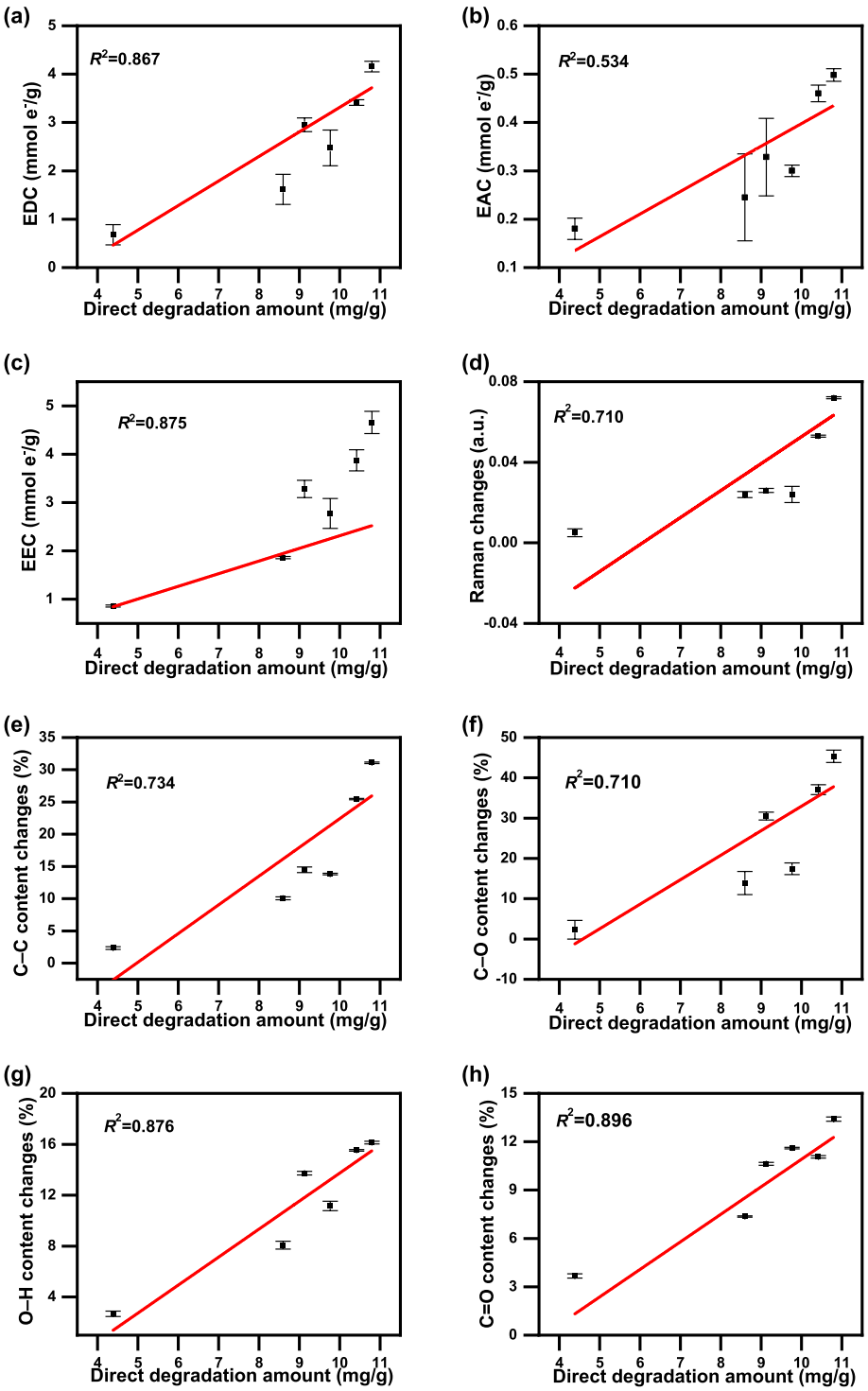

Fig. 8 The correlation between direct degradation amounts and (**a**) EDC, (**b**) EAC, (**c**) EEC, (**d**) Raman changes, (**e**) C–C content changes, (**f**) C–O content changes, (**g**) O–H content changes, (**h**) C=O content changes before and after the reaction

and indirect pathways. Direct electron transfer could be driven by oxygen-containing functional groups (C–O and O–H) and graphitic structure. The O–H groups could act as electron donors and form hydrogen bonds with electronegative atoms in pollutants or water molecules, shortening the electron transfer distance between

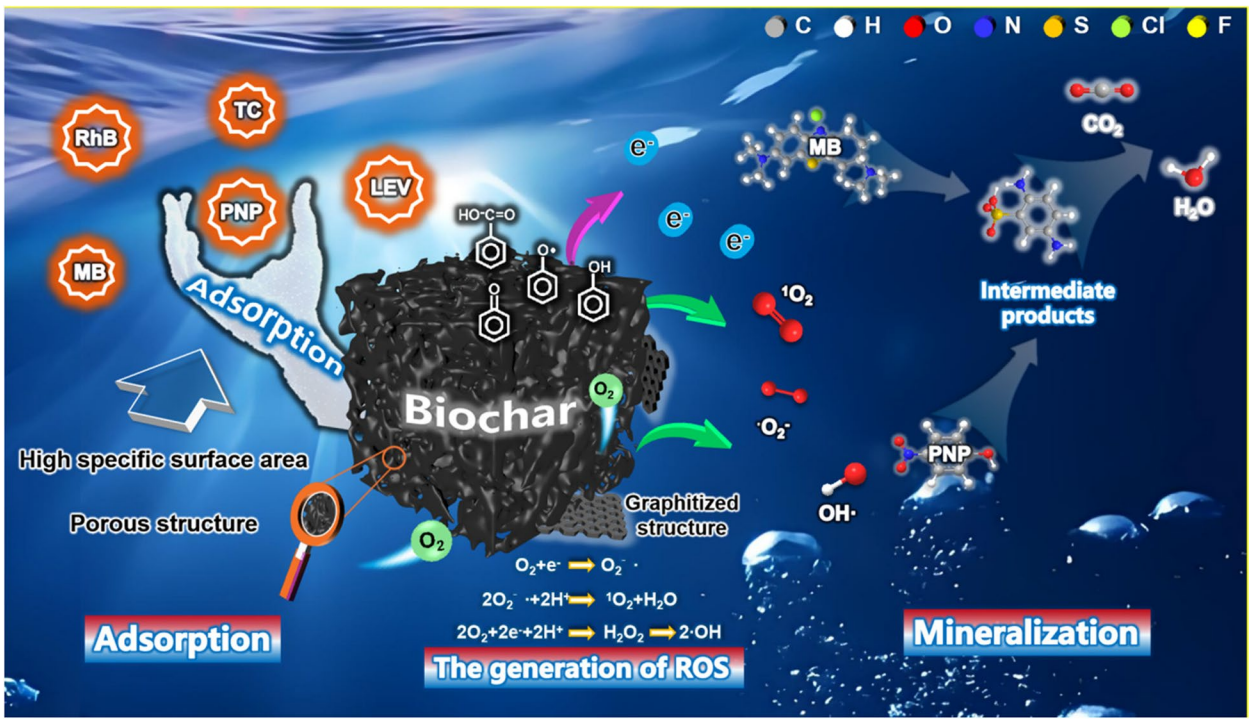

Fig. 9 Possible degradation mechanisms in biochar-organic system

biochar (donor) and pollutants (acceptor). Simultaneously, the C–O groups could participate in electron transfer through electrostatic interactions or hydrogen bonding, leveraging the electronegativity of oxygen atoms. The graphitic sp^2-carbon structure further enhanced the electron transfer efficiency via π-π stacking interactions with aromatic rings in pollutants, producing strong interfacial contact for redox reactions. Indirect degradation involved in the catalytic generation of ROS. For example, the surface functional groups could activate dissolved oxygen to produce $\cdot O_2^-$, which went through the proton-coupled dismutation to form H_2O_2 and $^1O_2$. Also, the persistent free radicals on biochar could directly excite ground-state oxygen into $^1O_2$ through energy transfer. This synergistic effect of direct electron transfer and radical-mediated reduction–oxidation endowed biochar with degradation capacity in the traditional adsorption process, which should be paid attention.

3.6 Stability of direct degradation ability of biochar

As the number of reaction cycles increased, the proportion of direct degradation in the overall degradation process gradually improved (Fig. 10). This trend was attributed to the gradual weakening of biochar's indirect degradation capacity. Reactive oxygen species, such as ·OH and $^1O_2$, were consumed during the cycling reactions. Although the absolute rate of direct degradation for APP-1 to APP-6 showed a declining trend, reflecting that the indirect degradation dominated in the former cycle. With the depletion of ROS, the relative contribution of direct degradation increased in spite of the decrease of whole removal efficiency. The enhancement of biochar performance was driven by structural evolution with the increasing of APP impregnation ratios, which promoted the formation of oxygen-rich functional groups for the generation of ROS and direct electron transfer.

3.7 Application potentiality and challenge

Recently, most of biochar materials are used as adsorbents to adsorb pollutants or as catalysts for oxidants (*e.g.* H_2O_2, persulfate, O_3) to degrade organic pollutants via free radical pathway. Moreover, ROS-dominated degradation pathways account for over 80% of pollutant removal, which may suffer from drastic efficiency loss in low-oxidant input or radical scavenging by the complicated constituents in natural water. In this study, we tried to figure out the direct degradation of organic pollutants by biochar without any oxidants, even including dissolved oxygen. The direct degradation performance of biochar was mainly derived from the electron-accepting capacity and electron-donating capacity for the electron transfer between the organic pollutants and biochar. And the electron transfer property relied on the biochar

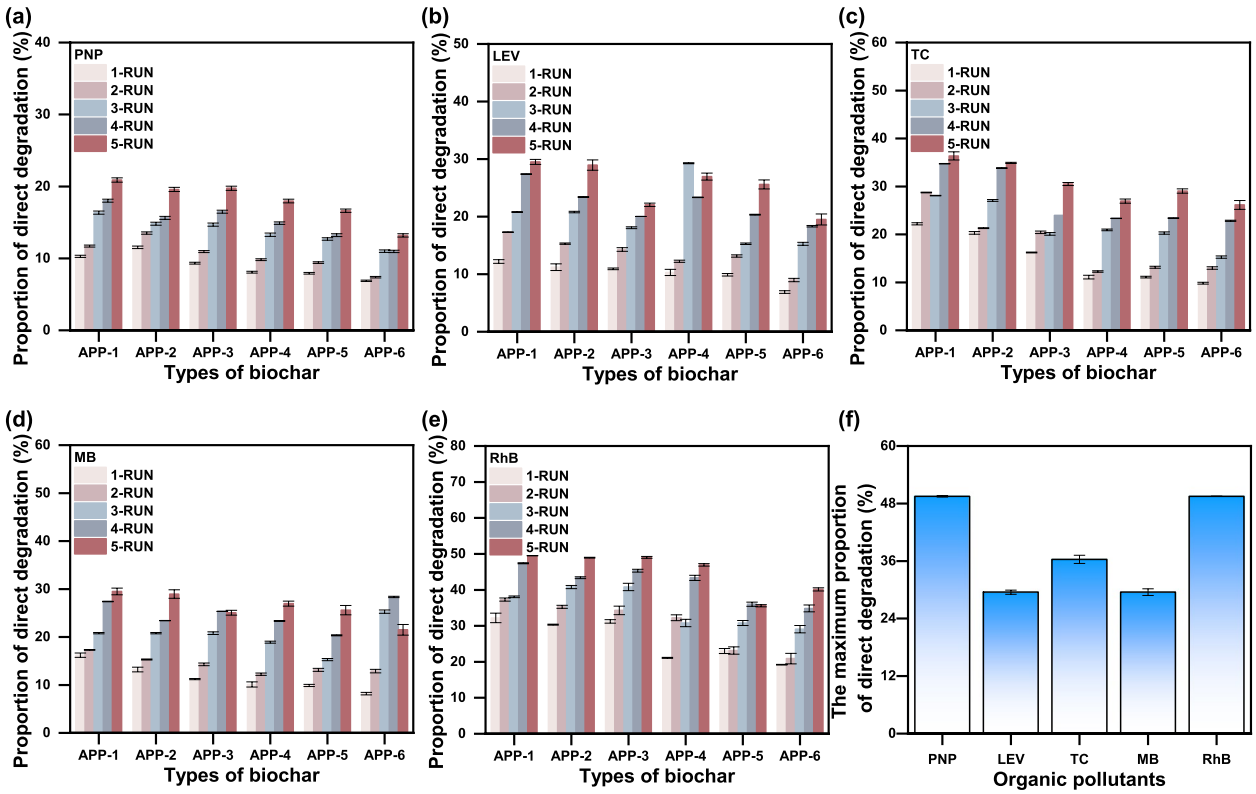

Fig. 10 Proportion of direct degradation of biochars for (**a**) PNP, (**b**) LEV, (**c**) TC, (**d**) MB, and (**e**) RhB; (**f**) The maximum direct degradation proportion of organic pollutants

characteristics, including surface functional groups, graphitization degree, π-π delocalization electron.

In this study, the APP-modified biochars exhibited a maximum direct degradation capacity of 11 mg/g, which was comparable to high-performance iron-based catalysts (15 mg/g) but without requiring acidic conditions or posing metal leaching risks (Fe^{3+} leaching > 2 ppm/cycle for iron catalysts) (Azmani et al. 2025; Li et al. 2023a, b; Yan et al. 2022). Moreover, the stability of direct degradation by biochar was also good enough. In a previous study, the iron-based materials suffered from an efficiency decline of 40% after 3 cycles due to passivation or leaching. Fortunately, the biochar kept higher than 90% degradation efficiency after 5 cycles via non-radical electron transfer pathways. Compared to photocatalysts, such as MOFs (30 mg/g) or TiO_2, biochar could operate the degradation process efficiently under dark conditions, eliminating energy-intensive light requirements and reducing operational costs. To be honest, although the direct degradation by biochar has some advantages, there were still some challenges. (1) The dissolved oxygen in natural water system may compete with the organic pollutants for the electrons from biochar, resulting in a reduction of direct degradation efficiency by 30% to 70% (Fig. 5). (2) The direct degradation of high redox potential pollutants by biochar might be hard, such as perfluoroalkyl and polyfluoroalkyl substances. In other words, the direct degradation by biochar is unlikely to cover all the organic pollutants recently. (3) The direct degradation performance in the really field-scale should be investigated in deep. As we all know, the real wastewater is normally complicated with a lot of interferent matters, such as humic organic matter, heavy metals.

4 Conclusions

The direct degradation performance of biochar was investigated with five different types of organic pollutants as examples. The results show that the direct degradation capability of biochar was governed by the oxygen-containing surface functional groups, specifically C–O and O–H moieties. These groups worked as electron donors to directly transfer electrons between the organic pollutants and biochar through dual pathways, namely hydrogen bonding with electronegative atoms and electrostatic interactions at redox-active interfaces. The characterization and correlation analyses revealed that the graphitic structure of biochar could enhance the electron transfer

between biochar and pollutants, significantly promoting direct degradation efficiency. Furthermore, the quenching experiments confirmed that biochar could indirectly degrade pollutants by catalyzing dissolved oxygen in water to generate ROS, such as ·OH and $^1O_2$. In other words, there were both direct degradation and indirect degradation in the natural water system, and the dissolved oxygen in natural water system may compete with the organic pollutants for the electrons from biochar. It is worth noting that both oxidation and reduction of the organic pollutants occurred during the direct degradation process. In our study, the optimal direct degradation performance of biochar could reach up to 11 mg/g, which contributed to 40% ± 10% of the total degradation. And the degradation contributed to approximately 30% ± 10% for overall removal performance, including both adsorption and potential degradation. Therefore, the direct degradation capability by biochar via direct electron transfer during the traditional adsorption should not be overlooked. This study provides a new insight into the property of biochar in wastewater treatment, rather than adsorbent or catalyst.

Supplementary Information

The online version contains supplementary material available at https://doi.org/10.1007/s44246-025-00219-3.

Supplementary Material 1.

Authors' contributions

All authors have contributed to the conception and design of this study. Material preparation, data collection, and analysis will be carried out by Fan Zhang. Yuan Gao, Rui Han, and Yajie Gao revised the manuscript. The author of the first draft is Zhang Fan, and all authors have provided comments on previous versions of the manuscript. All authors have read and approved the final manuscript.

Funding

This work was supported by National Natural Science Foundation of China (Grant numbers 52270059), and Natural Science Foundation of Liaoning Province of China (Grant numbers 2023-MS-095).

Data availability

The datasets used or analyzed during the current study are available from the corresponding author on reasonable requests.

Declarations

Competing interests

The authors declare that they have no known competing financial interests or personal relationships that could have appeared to influence the work reported in this paper.

Received: 4 February 2025 Revised: 9 April 2025 Accepted: 29 April 2025
Published online: 10 July 2025

References

Alsawy T, Rashad E, El-Qelish M, Mohammed RH (2022) A comprehensive review on the chemical regeneration of biochar adsorbent for sustainable wastewater treatment. NPJ Clean Water 5(1):1–21. https://doi.org/10.1038/s41545-022-00172-3

Azmani K, Besora M, Yu J, Teillout A, de Oliveira P, Mbomekallé I, Soriano-López J, Poblet JM, Galán-Mascarós J (2025) Water oxidation electrocatalysis in Acidic Media with Fe-Containing POMs/Carbon Composites. Inorg Chem 64(9):4260–4266. https://doi.org/10.1021/acs.inorgchem.4c04422

Beryani A, Flanagan K, You S, Forsberg F, Viklander M, Blecken G (2025) Critical field evaluations of biochar-amended stormwater biofilters for PFAS and other organic micropollutant removals. Water Res 281:123547. https://doi.org/10.1016/j.watres.2025.123547

Chen Q, Ma C, Duan W, Lang D, Pan B (2020) Coupling adsorption and degradation in p-nitrophenol removal by biochars. J Clean Prod 271:122550. https://doi.org/10.1016/j.jclepro.2020.122550

Chen X, Zhu J, Ma Y, Zeng C, Mu R, Deng Z, Zhang Z (2024) Facile synthesis of ball-milling and oxalic acid co-modified sludge biochar to efficiently activate peroxymonosulfate for sulfamethoxazole degradation: $^1O_2$ and surface-bound radicals. J Hazard Mater 465:133026. https://doi.org/10.1016/j.jhazmat.2023.133026

Chen H, Gao Y, Li J, Sun C, Sarkar B, Bhatnagar A, Bolan N, Yang X, Meng J, Liu Z, Hou H, Wong JWC, Hou D, Chen W, Wang H (2022) Insights into simultaneous adsorption and oxidation of antimonite [Sb (III)] by crawfish shell-derived biochar: spectroscopic investigation and theoretical calculations. Biochar 4(1). https://doi.org/10.1007/s42773-022-00161-2

Chu D, Dong H, Li Y, Jin Z, Xiao J, Xiang S, Dong Q, Hou X (2022) Enhanced activation of sulfite by a mixture of zero-valent Fe-Mn bimetallic nanoparticles and biochar for degradation of sulfamethazine in water. Sep Purif Technol 285:120315. https://doi.org/10.1016/j.seppur.2021.120315

Cui X, Wang J, Wang X, Du G, Khan KY, Yan B, Cheng Z, Chen G (2022) Pyrolysis of exhausted hydrochar sorbent for cadmium separation and biochar regeneration. Chemosphere 306:135546. https://doi.org/10.1016/j.chemosphere.2022.135546

Deng J, Han J, Hou C, Zhang Y, Fang Y, Du W, Li M, Yuan Y, Tang C, Hu X (2023) Efficient removal of per- and polyfluoroalkyl substances from biochar composites: Cyclic adsorption and spent regenerant degradation. Chemosphere 341:140051. https://doi.org/10.1016/j.chemosphere.2023.140051

Dong S, Xu W, Guo Q, Luo K, Cheng H, Tang J, Wang D, He Z, Wang L, Song S, Ma J (2024) Enhanced 2, 6-dimethylpyrazine removal by catalytic ozonation with legumes biochar: the roles of oxygen- and nitrogen-containing functional groups. Sep Purif Technol 334:125991. https://doi.org/10.1016/j.seppur.2023.125991

Egyir M, Luyima D, Park S, Lee KS, Oh T (2022) Volatilisations of ammonia from the soils amended with modified and nitrogen-enriched biochars. Sci Total Environ 835:155453. https://doi.org/10.1016/j.scitotenv.2022.155453

Fang G, Liu C, Wang Y, Dionysiou DD, Zhou D (2017) Photogeneration of reactive oxygen species from biochar suspension for diethyl phthalate degradation. Appl Catal B 214:34–45. https://doi.org/10.1016/j.apcatb.2017.05.036

Feng S, Zhang P, Duan W, Li H, Chen Q, Li J, Pan B (2020) P-nitrophenol degradation by pine-wood derived biochar: the role of redox-active moieties and pore structures. Sci Total Environ 741:140431. https://doi.org/10.1016/j.scitotenv.2020.140431

Feng G, Li W, Ye H, Wang T, Liu Y, Jing B, Nie C, Li D, Ao Z (2025) Molten salt-assisted synthesis of a nitrogen-doped biochar catalyst at low temperature for enhanced degradation of acetaminophen. J Mater Chem a 13(4):2677–2689. https://doi.org/10.1039/D4TA07221A

Fu X, Niu X, Zhang D, Li L, Ye X, Liao S, Li M, Lao C, Chen D, Lin Y, Yang Z (2024) Insights into novel phosphorus-doped biochar for tetracycline removal: Non-radical oxidation and adsorption. J Environ Chem Eng 12(6):114224. https://doi.org/10.1016/j.jece.2024.114224

Gorski CA, Klüpfel L, Voegelin A, Sander M, Hofstetter TB (2012) Redox Properties of Structural Fe in Clay Minerals. 2. Electrochemical and Spectroscopic Characterization of Electron Transfer Irreversibility in Ferruginous Smectite, SWa-1. Environ Sci Technol 46(17):9369–9377. https://doi.org/10.1021/es302014u

Govindan M, Adam Gopal R, Moon IS (2020) Electrochemical sequential reduction and oxidation facilitates the continual ambient temperature degradation of SF_6 to nontoxic gaseous compounds. Chem Eng J 382:122881. https://doi.org/10.1016/j.cej.2019.122881

Guo D, Wu J, Feng D, Zhang Y, Zhu X, Luo Z, Kang Y, Zhao Y, Sun S (2023) Mechanism of efficient magnetic biochar for typical aqueous organic

contaminant combined-adsorption removal. Fuel Process Technol 247:107795. https://doi.org/10.1016/j.fuproc.2023.107795
Hou J, Yu J, Li W, He X, Li X (2022) The Effects of Chemical Oxidation and High-Temperature Reduction on Surface Functional Groups and the Adsorption Performance of Biochar for Sulfamethoxazole Adsorption. Agronomy 12(2):510. https://doi.org/10.3390/agronomy12020510
Hoving AL, Sander M, Bruggeman C, Behrends T (2017) Redox properties of clay-rich sediments as assessed by mediated electrochemical analysis: Separating pyrite, siderite and structural Fe in clay minerals. Chem Geol 457:149–161. https://doi.org/10.1016/j.chemgeo.2017.03.022
Huang R, Feng T, Wu S, Zhang X, Fan Z, Yu Q, Chen Y, Chen T (2023) In-situ synthesis of magnetic iron-chitosan-derived biochar as an efficient persulfate activator for phenol degradation. Environ Res 234:116604. https://doi.org/10.1016/j.envres.2023.116604
Huang J, Zheng H, Xu H, Mo Q, Zhang X, Sheng G (2025) Magnetic bimetallic Fe and Cu-loaded N-doped biochar for the activation of peroxomonosulfate for tetracycline degradation: DFT calculations and mechanism analysis. Appl Surf Sci 679:161158. https://doi.org/10.1016/j.apsusc.2024.161158
Kang H, Ren H, Labidi A, Liao Y, Wang Y, Zheng H, Bahnemann D, Wang C (2025) Fe_3O_4 loaded biochar to enhance persulfate activation for tetracycline degradation: Performance and mechanism. Chemosphere 376:144267. https://doi.org/10.1016/j.chemosphere.2025.144267
Li H, Liu Y, Jiang F, Bai X, Li H, Lang D, Wang L, Pan B (2022a) Persulfate adsorption and activation by carbon structure defects provided new insights into ofloxacin degradation by biochar. Sci Total Environ 806:150968. https://doi.org/10.1016/j.scitotenv.2021.150968
Li M, Li D, Guan Z, Xu Q, Shi Y, Xia D (2022b) Carboxy-functionalized sludge-derived biochar for efficiently activating peroxymonosulfate to degrade bisphenol A. Sep Purif Technol 297:121525. https://doi.org/10.1016/j.seppur.2022.121525
Li S, Liu Y, Zheng H, Niu J, Leong YK, Lee D, Chang J (2023a) Biochar loaded with $CoFe_2O_4$ enhances the formation of high-valent Fe (IV) and Co (IV) and oxygen vacancy in the peracetic acid activation system for enhanced antibiotic degradation. Bioresour Technol 387:129536. https://doi.org/10.1016/j.biortech.2023.129536
Li T, Pan J, Wang X, Fan Z, Shi T, Wang L, Gao B (2023b) Insights into the fundamental role of Mo doping in facilitating the activation of peroxydisulfate by iron-based catalysts: Accelerating the generation of sulfate radicals. Chem Eng J 477:147000. https://doi.org/10.1016/j.cej.2023.147000
Li B, Wang C, Li N, Chen C, Zhu Z, Tang X, Cui Y, Liu T, Attatsi CK, Wang X (2024) Partially oxidized mackinawite/biochar for photo-fenton organic contaminant removal: Synergistically improve interfacial electron transfer and H_2O_2 activation. Environ Pollut 346:123660. https://doi.org/10.1016/j.envpol.2024.123660
Liang J, Duan X, Xu X, Chen K, Zhang Y, Zhao L, Qiu H, Wang S, Cao X (2021) Persulfate Oxidation of Sulfamethoxazole by Magnetic Iron-Char Composites via Nonradical Pathways: Fe (IV) Versus Surface-Mediated Electron Transfer. Environ Sci Technol 55(14):10077–10086. https://doi.org/10.1021/acs.est.1c01618
Liu F, Ding J, Zhao G, Zhao Q, Wang K, Wang G, Gao Q (2022) Catalytic pyrolysis of lotus leaves for producing nitrogen self-doping layered graphitic biochar: performance and mechanism for peroxydisulfate activation. Chemosphere 302:134868. https://doi.org/10.1016/j.chemosphere.2022.134868
Miao X, Chen X, Wu W, Lin D, Yang K (2022) Intrinsic defects enhanced biochar/peroxydisulfate oxidation capacity through electron-transfer regime. Chem Eng J 438:135606. https://doi.org/10.1016/j.cej.2022.135606
Mon PP, Cho PP, Chandana L, Srikanth VVSS, Madras G, Ch S (2023) Biowaste-derived Ni/NiO decorated-2D biochar for adsorption of methyl orange. J Environ Manage 344:118418. https://doi.org/10.1016/j.jenvman.2023.118418
Ouiriemmi I, Escudero-Curiel S, Pazos M, Angeles Sanromán M (2022) On-site regeneration by ultrasound activated persulfate of iron-rich Antipyrine-loaded biochar. J Environ Chem Eng 10(5):108400. https://doi.org/10.1016/j.jece.2022.108400
Shao F, Xu J, Kang X, Hu Z, Shao Y, Lu C, Zhao C, Ren Y, Zhang J (2023) An attempt to enhance the adsorption capacity of biochar for organic pollutants - characteristics of $CaCl_2$ biochar under multiple design conditions. Sci Total Environ 854:158675. https://doi.org/10.1016/j.scitotenv.2022.158675
Sun J, Zhang D, Xia D, Li Q (2023) Orange peels biochar doping with Fe-cu bimetal for PMS activation on the degradation of bisphenol a: a synergy of $SO_4^{\bullet-}$, ·OH, $^1O_2$ and electron transfer. Chem Eng J 471:144832. https://doi.org/10.1016/j.cej.2023.144832
Tian S, Jiang S, Xu Y, Ma J, Wen G (2025) New insight into enhanced permanganate oxidation by lignocellulose-derived biochar: the overlooked role of persistent free radicals. Water Res 274:123069. https://doi.org/10.1016/j.watres.2024.123069
Wang H, Guo W, Liu B, Wu Q, Luo H, Zhao Q, Si Q, Sseguya F, Ren N (2019) Edge-nitrogenated biochar for efficient peroxydisulfate activation: an electron transfer mechanism. Water Res 160:405–414. https://doi.org/10.1016/j.watres.2019.05.059
Wang S, Luo F, He L, Liu Z, Wang J, Liao Z, Hou H, Li J, Ning X, Chen Z (2025) Enhanced sludge dewaterability and confined antibiotics degradation in biochar-mediated chemical conditioning through modulating Fe oxidative states distribution and reaction sites in multiphase. Water Res 270:122789. https://doi.org/10.1016/j.watres.2024.122789
Wu D, Chen Q, Wu M, Zhang P, He L, Chen Y, Pan B (2022) Heterogeneous compositions of oxygen-containing functional groups on biochars and their different roles in Rhodamine B degradation. Chemosphere 292:133518. https://doi.org/10.1016/j.chemosphere.2022.133518
Wu W, Wang R, Chang H, Zhong N, Zhang T, Wang K, Ren N, Ho S (2023a) Rational electron tunning of magnetic biochar via N, S Co-doping for intense tetracycline degradation: efficiency improvement and toxicity alleviation. Chem Eng J 458:141470. https://doi.org/10.1016/j.cej.2023.141470
Wu Y, Zhang P, Zhang PJ, Feng S, Du W, Li H, Pan B (2023b) The degradation of p-nitrophenol by biochar is dominated by its electron donating capacity. Sci Total Environ 902:166115. https://doi.org/10.1016/j.scitotenv.2023.166115
Wu Y, Wang Z, Yan Y, Zhou Y, Huma B, Tan Z, Zhou T (2024) Recovery and regeneration of water-hardened magnetic composite biochar sphere for the removal of multiple heavy metals in contaminated soils. J Clean Prod 450:141906. https://doi.org/10.1016/j.jclepro.2024.141906
Xiao H, Wang Y, Lv K, Zhu C, Guan X, Xie B, Zou X, Luo X, Zhou Y (2025) N-doped biochar-Fe/Mn as a superior peroxymonosulfate activator for enhanced bisphenol a degradation. Water Res 278:123399. https://doi.org/10.1016/j.watres.2025.123399
Yan B, Shi Z, Lin J, Zhang L, Han L, Shi X, Yang Q (2022) Boosting heterogeneous fenton reactions for degrading organic dyes via the photothermal effect under neutral conditions. Environ Sci Nano 9(2):532–541. https://doi.org/10.1039/D1EN00874A
Yang J, Pan B, Li H, Liao S, Zhang D, Wu M, Xing B (2016) Degradation of *p* -nitrophenol on biochars: role of persistent free radicals. Environ Sci Technol 50(2):694–700. https://doi.org/10.1021/acs.est.5b04042
Yang J, Pignatello JJ, Pan B, Xing B (2017) Degradation of *p* -nitrophenol by lignin and cellulose chars: H_2O_2 -mediated reaction and direct reaction with the char. Environ Sci Technol 51(16):8972–8980. https://doi.org/10.1021/acs.est.7b01087
Yang Y, Cui Y, Zhao K, Sun H, Zhang W, Kuang P, Ma X, Zhu K, Ma K (2025a) Unleashing the potential of biomass-doped sludge biochar: promotion of persulfate activation by biochar-derived dissolved organic matter. Sep Purif Technol 361:131468. https://doi.org/10.1016/j.seppur.2025.131468
Yang Y, Jian Y, He L (2025b) High performance persistent organic pollutants removal using stabilized enzyme aggregates over amino functionalized magnetic biochar. J Hazard Mater 491:137868. https://doi.org/10.1016/j.jhazmat.2025.137868
Yin Q, Yan H, Liang Y, Jiang Z, Wang H, Nian Y (2023) Activation of persulfate by blue algae biochar supported FeO_X particles for tetracycline degradation: performance and mechanism. Sep Purif Technol 319:124005. https://doi.org/10.1016/j.seppur.2023.124005
Zeng L, Chen Q, Tan Y, Lan P, Zhou D, Wu M, Liang N, Pan B, Xing B (2021) Dual roles of biochar redox property in mediating 2,4-dichlorophenol degradation in the presence of Fe^{3+} and persulfate. Chemosphere 279:130456. https://doi.org/10.1016/j.chemosphere.2021.130456
Zhang K, Sun P, Khan A, Zhang Y (2021) Photochemistry of biochar during ageing process: Reactive oxygen species generation and benzoic acid degradation. Sci Total Environ 765:144630. https://doi.org/10.1016/j.scitotenv.2020.144630
Zhang Y, Tan X, Lu R, Tang Y, Qie H, Huang Z, Zhao J, Cui J, Yang W, Lin A (2023) Enhanced removal of polyfluoroalkyl substances by simple modified biochar: adsorption performance and theoretical calculation. ACS ES&T Water 3(3):817–826. https://doi.org/10.1021/acsestwater.2c00597

Zhang X, Sun W, Wang Y, Li Z, Huang X, Li T, Wang H (2024b) Mechanochemical synthesis of microscale zero-valent iron/N-doped graphene-like biochar composite for degradation of tetracycline via molecular O_2 activation. J Colloid Interface Sci 659:1015–1028. https://doi.org/10.1016/j.jcis.2024.01.061

Zhang X, Hou J, Zhang S, Cai T, Liu S, Hu W, Zhang Q (2024) Standardization and micromechanistic study of tetracycline adsorption by biochar. Biochar 6(1). https://doi.org/10.1007/s42773-023-00299-7

Zhu B, Liu J, Shen Y, Liu L, Liu F (2025a) The bidirectional matter transfer in adsorption-promoted photocatalytic ozonation system derived by triazine nanosheets-heptazine nanotubes homojunction composite biochar. Water Res 279:123444. https://doi.org/10.1016/j.watres.2025.123444

Zhu H, Ma H, Zhao Z, Xu L, Li M, Liu W, Lai B, Vithanage M, Pu S (2025b) Electron transfer tuning for persulfate activation via the radical and non-radical pathways with biochar mediator. J Hazard Mater 486:136825. https://doi.org/10.1016/j.jhazmat.2024.136825

Zhu Z, Gou Q, Duan W, Chen F, Steinberg CEW, Pan B. (2025). Biochar-mediated degradation of p-nitrophenol as influenced by species of Fe(III). Biochar, 7(1). https://doi.org/10.1007/s42773-025-00448-0

Publisher's Note